Research Article

Journal of Molecular Recognition

Received: 23 March 2009, Revised: 3 August 2009, Accepted: 15 September 2009, Published online in Wiley InterScience: 25 November 2009

(www.interscience.wiley.com) DOI:10.1002/jmr.999

Interaction of p53 with Mdm2 and azurin as studied by atomic force spectroscopy

Gloria Funari[a], Fabio Domenici[a], Lavinia Nardinocchi[b,c], Rosa Puca[b,c], Gabriella D'Orazi[b,c], Anna Rita Bizzarri[a] and Salvatore Cannistraro[a]*

Azurin, a bacterial protein, can be internalized in cancer cells and induce apoptosis. Such anticancer effect is coupled to the formation of a complex with the tumour-suppressor p53. The mechanism by which azurin stabilizes p53 and the binding sites of their complex are still under investigation. It is also known that the predominant mechanism for p53 down-regulation implies its association to Mdm2, the main ubiquitin ligase affecting its stability. However, the p53/Mdm2 interaction, occurring at the level of both their N-terminal domains, has been characterized so far by experiments involving only partial domains of these proteins. The relevance of the p53/Mdm2 complex as a possible target of the anticancer therapies requires a deeper study of this complex as made up of the two entire proteins. Moreover, the apparent antagonist action of azurin against Mdm2, with respect of p53 regulation, might suggest the possibility that azurin binds p53 at the same site of Mdm2, preventing in such a way p53 and Mdm2 from association and thus p53 from degradation. By following the interaction of the two entire proteins by atomic force spectroscopy, we have assessed the formation of a specific complex between p53 and Mdm2. We found for it a binding strength and a dissociation rate constant typical of dynamical protein–protein interactions and we observed that azurin, even if capable to bind p53, does not compete with Mdm2 for the same binding site on p53. The formation of the p53/Mdm2/azurin ternary complex might suggest an alternative anti-cancer mechanism adopted by azurin.

Supporting information may be found in the online version of this paper.

Keywords: p53; Mdm2; azurin; force spectroscopy; molecular interaction; AFM

INTRODUCTION

p53, 'the guardian of the genome', is probably the most extensively characterized transcription factor with a tumour-suppressor activity (Oren, 2003; Harris and Levine, 2005). The human p53 protein consists of four major domains which are responsible for its transcriptional activation DNA-binding and tetramerization functions (Ko and Prives, 1996; Levine, 1997). In presence of different stress signals, p53 is stabilized through post-translational modifications (Lavin and Gueven, 2006), its cellular levels increase and it can induce the expression of its target genes that, in turn, control the process of DNA-repair, the cell-cycle arrest and the apoptotic cascade (Vogelstein *et al*., 2000).

The activity of p53 is down regulated by the cellular oncoprotein Mdm2 (Freedman *et al*., 1999) that promotes its ubiquitin-dependent degradation (Honda *et al*., 1997), inhibits its transcriptional function (Momand *et al*., 1992) and exports it from the nucleus to the cytoplasm (Roth *et al*., 1998). The action of Mdm2 has been demonstrated to be coupled with the formation of a complex with p53 (Momand *et al*., 1992). However, detailed information on the overall structure of the corresponding complex is missing to date, mainly due to the presence, within both proteins, of large unstructured regions (Bell *et al*., 2002; Dawson *et al*., 2003) that prevent the entire complex from crystallization. The only piece of structural and kinetic information available to date derives from studies performed on partial domains of both p53 and Mdm2 (Kussie *et al*., 1996; Lai *et al*., 2000; Schon *et al*., 2002; Chi *et al*., 2005).

Undoubtedly, a study involving the two entire proteins would be better suited for a more realistic and comprehensive knowledge about their interaction. Moreover, the importance of investigating this interaction is not limited to structural or kinetic aspects: due to the role of p53 on cellular equilibrium and integrity, it represents a central target for a variety of attractive anticancer strategies with the common aim at stabilizing and enhancing p53 tumour-suppression function (Vassilev *et al*., 2004; Wiman, 2006; Bossi and Sacchi, 2007; Vassilev, 2007).

In this connection, it has been reported that azurin, a copper-containing protein with electron-transfer activity in

* *Correspondence to: S. Cannistraro, Biophysics and Nanoscience Centre, Facoltà di Scienze, Università della Tuscia; Largo dell'Università, 01100 Viterbo, Italy.*
E-mail: cannistr@unitus.it

a *G. Funari, F. Domenici, A. R. Bizzarri, S. Cannistraro*
Biophysics and Nanoscience Centre, CNISM, Facoltà di Scienze, Università della Tuscia, Viterbo, Italy

b *L. Nardinocchi, R. Puca, G. D'Orazi*
Molecular Oncogenesis Laboratory, Regina Elena Cancer Institute, Rome, Italy

c *G. D'Orazi*
Department of Oncology and Neurosciences, University 'G. D'Annunzio', Chieti, Italy

Pseudomonas Aeruginosa (Vijgenbbom *et al*., 1997), plays an anticancer role, as observed in different cell lines: it can enter cancer cells and induce their apoptotic death *in vitro* and *in vivo* (Yamada *et al*., 2002). Interestingly, it has been demonstrated that the pro-apoptotic action of azurin on cancer cells is concomitant with the formation of a complex with p53, thereby leading to both its stabilization and its intracellular level increase.

In this connection, the p53/azurin complex has been subjected to different experimental investigations (Yamada *et al*., 2002; Apiyo and Wittung-Stafshede, 2005; Taranta *et al*., 2008a).

Site-direct mutagenesis (Yamada *et al*., 2002) has shown that azurin interacts through two methionine residues located within its hydrophobic patch surrounding the copper atom, with a not univocally established portion of p53. Two different docking computational studies have predicted that azurin could interact with the DNA-binding domain (DBD) of p53 (De Grandis *et al*., 2007) or, alternatively, contact its N-terminal region (Taranta *et al*., 2008b). The latter possibility is also suggested by an experimental fluorescence work (Apiyo and Wittung-Stafshede, 2005). Nevertheless, even if the molecular mechanism underlying the action of azurin has to be completely elucidated, the protein is undoubtedly capable to stabilize p53, contrasting in such a way the negative regulation exerted by Mdm2. An appealing hypothesis to this end could be that azurin, by contacting the p53 N-terminal portion, might partially, or totally, cover the Mdm2-binding site on p53 and therefore prevent the two proteins from association and then p53 from degradation.

Before examining this working hypothesis, we have assessed the formation of the p53/Mdm2 complex involving the two entire proteins with atomic force spectroscopy (AFS). This innovative and powerful nano-technological methodology, able to investigate the strength and kinetics of bio-complexes, at the single-molecule level, in native conditions and without any label or sample preparation, has been widely employed in recent times to get detailed information on biological interactions (Ratto *et al*., 2004; Bonanni *et al*., 2005; Bonanni *et al*., 2006; Hinterdorfer and Dufrêne, 2006; Sulchek *et al*., 2006) We have found that a specific bio-recognition process occurs between p53 and Mdm2 when the full-length-protein interaction is studied at the single-molecule level by AFS. The measured binding strength and dissociation rate constant of the corresponding complex fall in the range of values typical of ligand/receptor interactions. Moreover, it has been observed that azurin, even if it is capable to strongly and specifically bind p53, does not appear to compete with Mdm2 for the same binding site.

MATERIALS AND METHODS

Protein expression and purification

Glutathione S-transferase (GST) fusions of human MDM2 (kindly provided by A. L. Haas, LSU Health Sciences Center, New Orleans, LA, USA) and human wild-type-p53 (kindly provided by S. Soddu, National Cancer Institute 'Regina Elena', Rome, Italy) were expressed in log phase *Escherichia coli* BL-21 that had been grown overnight at room temperature, diluted 1:20 in fresh Luria-Bertani medium containing 50 μg/ml ampicillin at 37°C with vigorous shaking. Isopropyl-1-thio-β-D-galactoside (IPTG) was added to a final concentration of 0.4 mM when the OD_{600} reached 0.4–0.8 value. Bacteria were harvested 3 h after addition of IPTG by centrifugation at 5000 rpm for 10 min. Cell pellets were resuspended with NENT buffer (Tris 20 mM at pH 8, NaCl 100 mM, EDTA 1 mM and NP40 0.5%), proteases inhibitors, phenylmethylsulfonylfluoride (PMSF) 1 μM and lysozyme and lysed by sonication. The sonicate was clarified by centrifugation at 4°C for 15 min at 5000 rpm and stored at −80°C. Levels of expressed GST fusion proteins were estimated by incubating sonicates with glutathione-Sepharose (GS) beads (Sigma), washing, and quantification by SDS-PAGE followed by staining with Comassie Brilliant Blue R-250. Known amounts of bovine serum albumine (BSA) were used as standards. Cleavage of the GST portion was achieved by digestion with thrombine CleaveClean kit (Sigma) according to the manufacturer's instructions. The quality, correct folding, and purity of the obtained proteins were assessed through structural and functional studies, as reported in the Supporting Material.

Tip functionalization

Silicon nitride cantilevers (Veeco Instruments, Santa Barbara, CA) used in the experiments consist of contact microlevers with backside gold coating and an oxide-sharpened tip. The tips were cleaned in acetone for 10 min, dried with a stream of nitrogen and then UV irradiated for 30 min. Tips were then immersed in a solution of 2% (v/v) 3-mercatopropyl-trimethoxysilane (Aldrich) in toluene, incubated for 2 h at room temperature, then extensively washed with toluene and dried with nitrogen. The silanized tips were immersed in a solution of 1 mM N-hydroxysuccinimide-polyethylenglycol-maleimide (NHS-PEG-MAL, MW 3400 Da, 30 ± 10 nm in length, from Nektar Therapeutics) in DMSO for 3 h at room temperature. This spacer contains a thiol-reactive group (MAL) at one end, to link silane molecules, and an amino-reactive group (NHS) at the other end, to couple $–NH_2$ groups of lysines exposed on the protein surface. Tips were then rinsed in three changes of DMSO to remove the unbound PEG. Eventually tips were incubated on parafilm, according to a protocol previously described (Ebner *et al*., 2007) with 50 μl of a 3.2 μM solution of Mdm2 (and, in alternative, a 10 μM solution of azurin, from Sigma) for 4 h at 4°C, then gently rinsed with buffer and stored in PBS at 4°C. The protocol used is sketched in Figure 1A.

Substrate preparation

The substrates used in our experiments consist of vacuum-evaporated thin gold film (250 nm in thickness) on borosilicate glass (Arrandee, Germany). These substrates were firstly flame-annealed (to obtain re-crystallized Au (111) terraces), immersed in a solution of 0.2 mM cisteamine (Sigma) in ethanol for 3 h at room temperature, then washed with ethanol and dried under a stream of nitrogen. The modified substrates were incubated with 100 μl of a solution of 1% glutaraldehyde (Sigma) in milliQ water for 10 min at room temperature, rinsed carefully with milliQ water and dried with nitrogen. For the protein immobilization, 50 μl of a solution of 1.2 μM p53-GST fusion protein were dropped on the amine-reactive surface of the substrates and incubated over-night at 4°C. Next day the substrates were gently washed and stored in milliQ water at 4°C. The protocol used is sketched in Figure 1B.

Imaging and force spectroscopy

The substrate imaging and the force measurements were performed with a Nanoscope IIIa/ Multimode atomic force

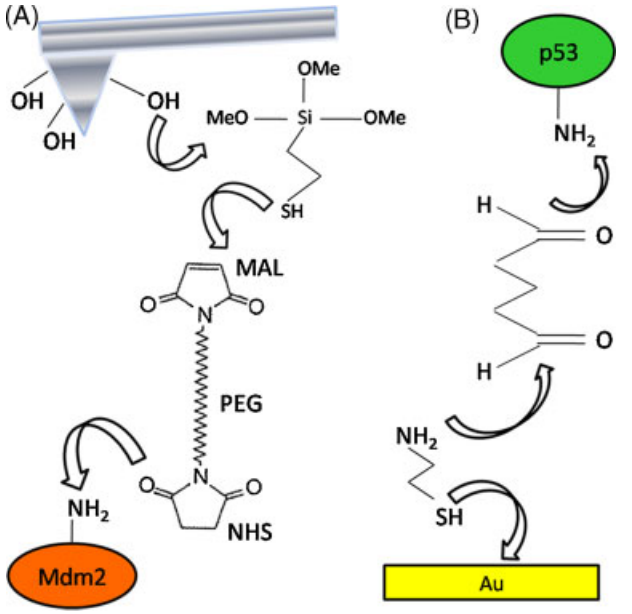

Figure 1. Schematic sketch of the surface chemistry employed to covalently anchor p53 and Mdm2 to AFM supports. (A) Mdm2 protein is bound to the mercapto-silanized tip via a 30 nm-long PEG chain. (B) p53 molecules are attached to a gold substrate via a chemical platform involving cisteamine and glutaraldehyde sequentially linked. Both p53 and Mdm2 are bound by randomly targeting aminic groups of lysine residues exposed on the protein surfaces. (For additional details see Materials and Methods section).

microscopy (AFM; Digital instruments, Santa Barbara, CA). Imaging of the p53 substrate was conducted in milliQ water by tapping mode AFM, with an amplitude set point corresponding to the 95% of the free amplitude value. The cantilever nominal spring constant, k_{nom}, was 0.5 N/m. Scratching of the substrate (to assess the presence of a single protein layer) was performed in contact mode AFM, by using a cantilever with a k_{nom} of 0.02 N/m. The applied force was varied from few nano-Newton for imaging to hundreds of nano-Newton for scratching. Force measurements were carried out in 50 mM (pH 7.2) PBS buffer by force calibration mode AFM. The cantilevers used to perform force measurements had k_{nom} of 0.02 and 0.03 N/m. The effective spring constants of the cantilevers, $k_{effective}$, calibrated using the non-destructive thermal noise method (Hutter and Bechhoefer, 1993), were in the range of 0.017–0.045 N/m. In all measurements a relative trigger of 23–35 nm was applied to limit at 0.7 nN the maximum contact force exerted on the protein monolayer by the tip, a ramp size of 150 nm was set and an encounter time (interval between approach and retraction phase) of 100 ms was established. The approach velocity was set, through the software actuating the piezo scan of our AFM Nanoscope IIIa, operating in open loop configuration, at a value of 69.8 nm/s, while the retraction velocity was changed from 50 to 8400 nm/s. Loading rates at which measurements were performed (instantaneous values, see Results and Discussion section) have been selected in the range 0.6–72 nN/s. All measurements performed for blocking experiments and competition experiments (see Results and Discussion section) were conducted at the same loading rate of 3 nN/s.

RESULTS AND DISCUSSION

p53/Mdm2 interaction

All experiments were performed by AFS, a single-molecule technique particularly useful to complement traditional proteomic and molecular biology approaches for the functional analysis of biological interactions (Zlatanova *et al*., 2000; Merkel, 2001; Rief and Grubmüller, 2002; Ratto *et al*., 2004; Bonanni *et al*., 2005; Bonanni *et al*., 2006; Hinterdorfer and Dufrêne, 2006; Sulchek *et al*., 2006; Taranta *et al*., 2008a). AFS is based on AFM, which operates by scanning a sharp tip mounted on a cantilever over a substrate. Inter-atomic forces, which are strongly dependent on tip-substrate distance, are measured by the cantilever deflection through the reflection of a laser beam from the back of the tip edge towards a photodiode. During the scan of the substrate (*xy* plane) the cantilever deflection is converted into height information to reproduce the surface topography. AFS exploits the principles of AFM to measure inter-atomic forces between the tip and the substrate at a fixed *xy* position. With reference to Figure 2, a ligand-functionalized tip is approached to a surface covered by immobilized receptors (point 1); at a given tip-sample distance the cantilever begins to deflect in consequence of intermolecular repulsive forces (point 2). From this point on, the cantilever exerts a pushing force on the substrate as evidenced by its deflection, while ligand and receptor, brought in close proximity, can interact and form a complex. The approach phase (dotted line) is stopped when the cantilever applies upon the substrate the maximum contact force (limited in order to avoid protein damage), having undergone an upward deflection, as shown in point 3. Next, the direction of motion is reversed and the cantilever retracts from the surface. During this retraction phase (continuous line) the cantilever reaches the baseline deflection and, by increasing further the tip-sample distance, it begins to bend downward (due to the attractive interaction-force displayed by the ligand–receptor complex, point 4). Its deflection follows a nonlinear course (curved tract) because of the stretching of the linker. When the force exerted by the cantilever overcomes the stability of the complex bonds, a sudden jump in the deflection occurs, as a consequence of the complex

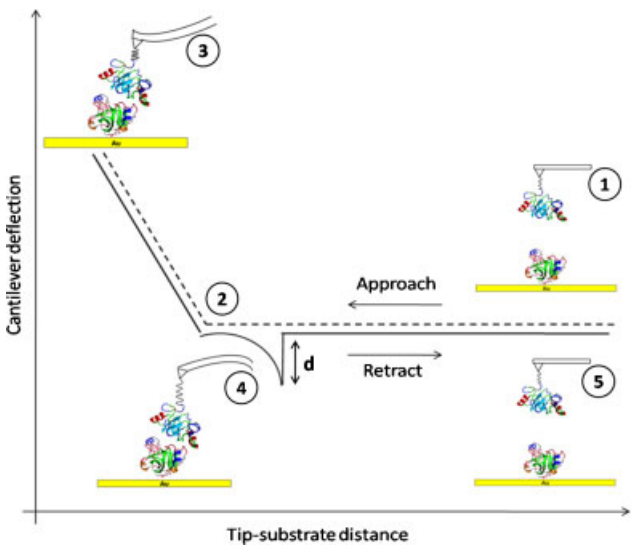

Figure 2. Sketch of AFS experiments. See text for a detailed description.

dissociation that separates the ligand–receptor pair (point 5). The deflection (d) measured at the jump-point is used to determine the force required to break the complex, the so called 'unbinding or rupture force', as the product between such deflection and the constant of the functionalized cantilever, by considering it as a spring governed by the Hooke law.

A fundamental prerequisite to investigate a ligand–receptor interaction by AFS is a robust attachment of ligand and receptor on their respective AFM supports, preferentially through covalent bonds, which are unquestionably stronger than those characteristics of protein-protein interactions (Hinterdorfer and Dufrêne, 2006). The strong immobilization of the two partners is useful to ensure the stability of the tethered system during time, by allowing repeated approach/retraction cycles.

Our immobilization strategy, described in details in Materials and Methods section, is schematically illustrated by the tethered system sketched in Figure 2 (point 1). Mdm2 was covalently fastened to the AFM tip via a flexible 30 nm-long polymer PEG (Figure 1A). The use of such a linker confers flexibility and provides the necessary re-orientational freedom for the occurrence of the bio-recognition between ligand and receptor (Friddle *et al*., 2007). Moreover, the linker spatially isolates non-specific tip-substrate adhesions, taking place near to the substrate surface, from the specific unbinding events of proteins that, being tethered, dissociate at larger tip-substrate distance (Hinterdorfer *et al*., 1996; Hinterdorfer *et al*., 2000).

p53 was covalently bound to a gold slide through a chemical platform composed by cisteamine and glutaraldehyde linked in sequence, to generate a protein monolayer on the substrate surface (Figure 1B).

Both partners were immobilized by targeting aminic groups exposed on the protein surfaces. The presence of several lysine residues available for the reaction (with glutaralheyde or NHS-group) generated different orientations of the proteins on tip and substrate, some of which might have been unfavourable for the bio-recognition event (see later).

Before proceeding with AFS measurements, we evaluated the aspect of p53 molecules immobilized on gold slide by tapping mode AFM with a bare tip. Figure 3 (left side) shows an AFM image corresponding to noticeable single protein molecules assembled to form a dense and uniform p53 layer. To assess the presence of a monolayer (of the expected height) we performed a scratch on it with the tip working in contact mode. As shown in Figure 3 (right side), the scratch depth was found to be about of 5 nm that corresponds to the expected thickness for a single protein layer and the cysteamine-glutaralheyde platform.

By repeating force-distance cycles on the tethered system sketched in Figure 2 (point 1), we collected thousands of force-curves. All curves were recorded at a constant approach speed, while the retraction velocity was varied from 50 to 8400 nm/s. To prevent protein damage, we fixed at 0.7 nN the value for the maximum contact force applied on the substrate. In these experimental conditions we performed measurements at several distinct points of the substrate by obtaining different kinds of force-curves. The most recurrent ones are shown in Figure 4. Curves that display acceptable unbinding events are collected in the left panel. They are characterized by: sharp peaks, starting and ending points at zero-deflection line, an initial nonlinear curved shape, due to the viscoelastic properties of a PEG molecule under stretching (Kienberger *et al*., 2000b; Thormann *et al*., 2006), and straight pull-off jumps. The right panel, instead, shows curves discarded from the analysis due to the lack of events or the presence of hysteresis or dubious deflection-jumps. Moreover, control experiments with a bare tip versus a p53-coated substrate and with a Mdm2-functionalized tip versus a bare substrate. Under these conditions we registered curves similar to those shown in Figure 4B.

The unbinding frequency, defined as the ratio between the number of accepted unbinding events and the totality of the collected force-curves, was found to be about 15% (at a loading rate of 3 nN/s). Such frequency was found to be consistent with values previously reported for other biological interactions (Sulchek *et al*., 2005; Fuhrmann *et al*., 2008). Even if a low unbinding frequency might originate also from the massive presence of unfolded or inactive proteins, we were led to exclude such a possibility on the basis of surface plasmon resonance checks with p53 covalently bound to a gold substrate, as for force spectroscopy measurements, that gave results (unpublished

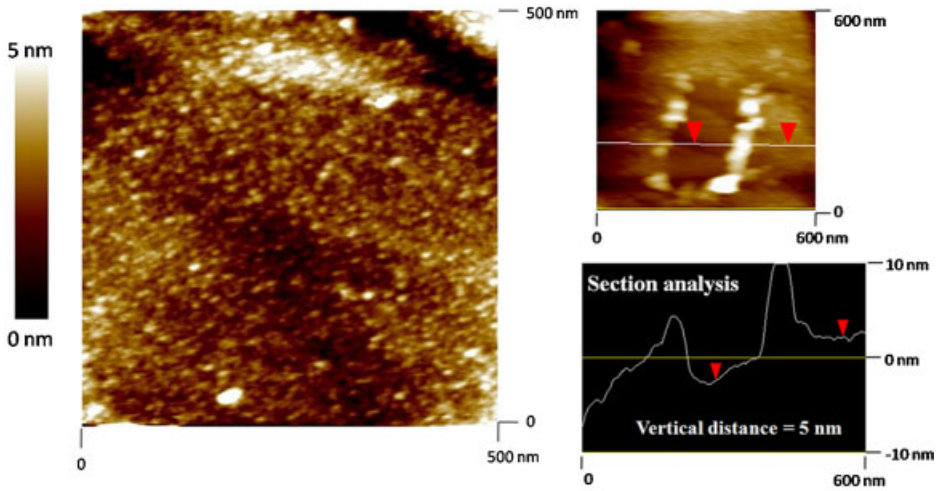

Figure 3. Left side: tapping mode AFM image of p53 monolayer on a gold substrate. The image has been recorded in milliQ water with an amplitude setpoint corresponding to the 95% of free amplitude value. Right side: contact mode AFM image of a scratching on p53 monolayer and the vertical profile analysis.

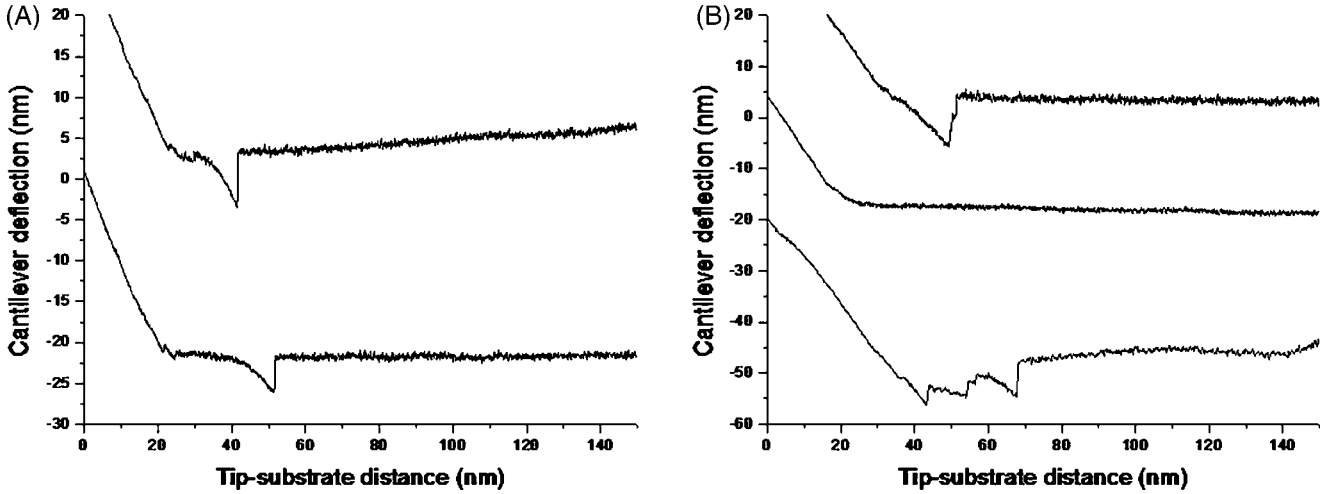

Figure 4. Representative examples of force-curves registered with a Mdm2-coated tip over a p53 protein monolayer (only the retraction traces are shown). The tip deflection (vertical axes) is plotted as a function of tip-substrate distance (abscissa axes). (A) Accepted curves containing specific unbinding events with sharp peak and nonlinear curved shape. (B) Rejected curves displaying adhesion (hysteresis), without events or with dubious adhesion events.

data) consistent with those obtained by force spectroscopy and in agreement with the literature (Schon *et al*., 2002). Rather, we believe that low unbinding frequencies could be due to the presence of unfavourable binding geometries and steric hindrance (Bonanni *et al*., 2005). Interestingly, the unbinding frequency was found to be dependent on the loading rate: it initially increased, reached a maximum and decreased thereafter, as already described (Lü *et al*., 2006).

As mentioned before, for each curve the unbinding force was determined as the product between the cantilever deflection (d) and its effective spring constant ($k_{effective}$). Accordingly, a number of force histograms, corresponding to the different loading rates at which the force spectroscopy measurements have been carried on, were generated. The histograms of the unbinding forces exhibit an almost single mode distribution with a skewness toward high force values; such an asymmetric shape, rather similar to that observed in other systems, can be due to several factors, such as multiple binding events, binding heterogeneity, etc (Baumgartner *et al*., 2000; Ratto *et al*., 2004; Sulchek *et al*., 2005). On such a basis, and in agreement with what commonly done in literature, we determined the most probable unbinding force from the maximum of the main peak of each histogram. At a loading rate of 3 nN/s, we found an unbinding force value of 105 ± 6 pN (Figure 5). This rupture force is in the range of values reported for other specific biological interactions at similar loading rates (Kienberger *et al*., 2000a; Zhang *et al*., 2002). The unbinding force values and the widths of their corresponding distributions increased with rising the loading rate, as observed in other force spectroscopy works (Janshoff and Steinem, 2001; Marshall *et al*., 2005).

Subsequently, to verify if the measured forces could be attributed to specific interaction events between p53 and Mdm2, we performed a blocking experiment on the complex. A solution of free Mdm2 was incubated on p53 substrate to allow the binding between p53 and the free molecules of Mdm2 to occur (Figure 6A). After incubation, we washed the substrate with buffer (to remove the unbound Mdm2) and we measured again the unbinding frequency with the same Mdm2-functionalized tip. Figure 6B shows a decrement from 15 to 5% of such unbinding frequency upon blocking. The significant reduction (of about 70%) observed after blocking is clearly indicative of the specificity of the p53/Mdm2 complex formation. The persistence of a residual unbinding activity (5%) upon blocking was observed also in other force spectroscopy experiments and could be related to the forced interaction between the two partners, induced by the experimental setup (Hinterdorfer *et al*., 1996; Wielert-Badt *et al*., 2002). Importantly, the force distributions before and after blocking (Figure 6C) showed a good overlap, thus indicating the same nature of the corresponding interactions.

Before describing the dissociation kinetics of the p53/Mdm2 complex by our force spectroscopy experiments, it is worth discussing, in more details, the general principles that govern the dissociation of a complex under the influence of an external force. In general, the application of a force to a complex until it

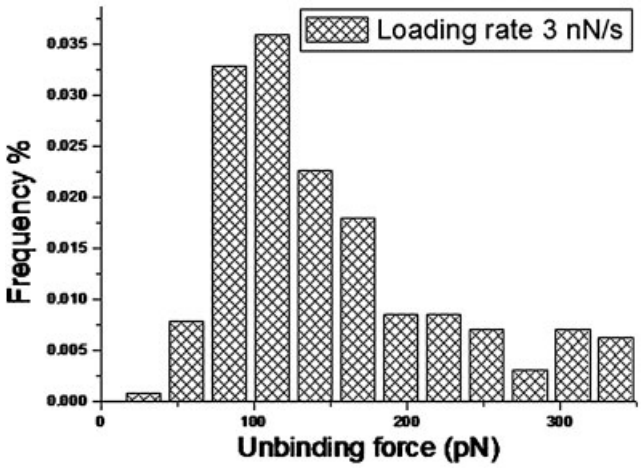

Figure 5. Unbinding force histogram for the p53/Mdm2 complex. The histogram was obtained by binning at 28 pN. The most probable unbinding force value was determined from the maximum of the main peak of each histogram. Data come from 210 unbinding events found within 1350 force curves, recorded at a loading rate of 3 nN/s.

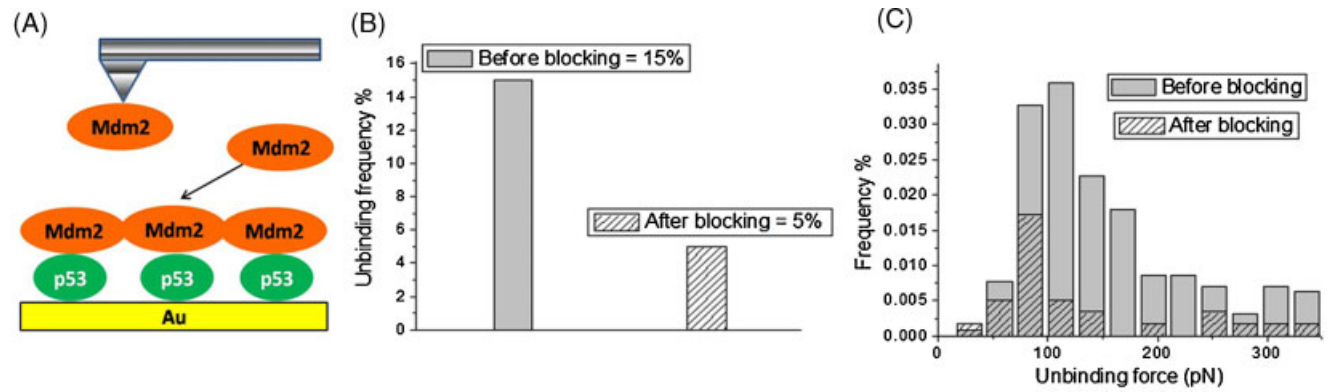

Figure 6. Blocking experiment. (A) A solution of free Mdm2 is incubated over the p53 monolayer. (B) Unbinding frequency between p53 and Mdm2 before and after blocking. (C) Unbinding force distributions before and after blocking. All measurements here illustrated are performed at a loading rate of 3 nN/s.

reaches the dissociated state renders the reaction a far-from equilibrium transformation that needs to be treated within an appropriate theoretical context. Bell-Evans model (Bell, 1978; Evans and Ritchie, 1997) represents the most widely used theory to explain and analyze force spectroscopy data. According to the model, the application of a force F on a complex toward the unbound state deforms the energy landscape of the ligand-receptor pair, leading to a reduction of the activation barrier and consequently in an exponential increase of the dissociation rate constant with the pulling force F, as follows:

$$k_{off}(F) = k_{off} \cdot \exp[F x_\beta/(k_B T)] \quad (1)$$

where k_{off} (F) and k_{off} are the dissociation rate constant in the presence and without any applied force respectively, x_β is the width of the potential barrier along the direction of the applied force, k_B is the Boltzmann's constant and T the absolute temperature. The effect of the applied force on the energy landscape distortion increases with raising the loading rate r_F at which the force is ramped. As a consequence the unbinding forces measured depend not only on the nature of the ligand-receptor interaction, but also on the rate at which the force is applied during time. As predicted by the model, in fact, the most probable rupture force F is a linear function of the natural logarithm of the loading rate r_F. Under conditions of constant loading rate r_F, the most probable unbinding force is given by the following expression:

$$F = (k_B T/x_\beta) \cdot \ln[r_F x_\beta/(k_{off}\, k_B\, T)] \quad (2)$$

Experimentally, F is determined from the maximum of the main peak of each force histogram, while for the loading rate it is considered the instantaneous value at the moment of bond rupture, determined as the product between the retraction speed and the spring constant of the entire system, k_{syst}. It is appropriate, in fact, to take into account the contribution of the spring constant of protein and linker molecules bound to the tip, by considering the k_{syst} parameter calculated from the slope of the retraction curve immediately prior to the unbinding event (Friedsam *et al.*, 2003).

By plotting the measured rupture forces versus the natural logarithm of the loading rate, we obtained a dynamic force spectrum displaying an evident linear relationship between the two quantities (Figure 7). The kinetic parameters x_β and k_{off}, at zero force conditions, were obtained by fitting the plot of F versus ln (r_F) with equation 2 and relate to the slope and intercept of the linear fit, respectively. Our dynamic force spectrum showed, at least in the range of the loading rates here taken in consideration, a single regime indicative of a single energy barrier and unique transition state of the reaction and provided values of 0.17 ± 0.01 nm for x_β and $1.5 \pm 0.5\ s^{-1}$ for k_{off}.

This k_{off} value falls within a range of values characteristic of several other ligand-receptor pairs, such as cadherins, selectins, integrins, etc. (Baumgartner *et al.*, 2000; Hanley *et al.*, 2003; Panorchan *et al.*, 2006; Friddle *et al.*, 2007; Lim *et al.*, 2008).

It is not surprising, on the other hand that the k_{off} value obtained for the p53/Mdm2 complex is found comparable to that of the above mentioned ligand-receptor pairs, rather to that of stronger complexes, such as antigen-antibody couples (with k_{off} going down to $10^{-10}\ s^{-1}$). Indeed, the cellular functionality of the p53/Mdm2 complex would more likely require a k_{off} typical of dynamical, transient interactions; for instance to allow, after the regulative association of Mdm2 to p53 for ubiquitination, the

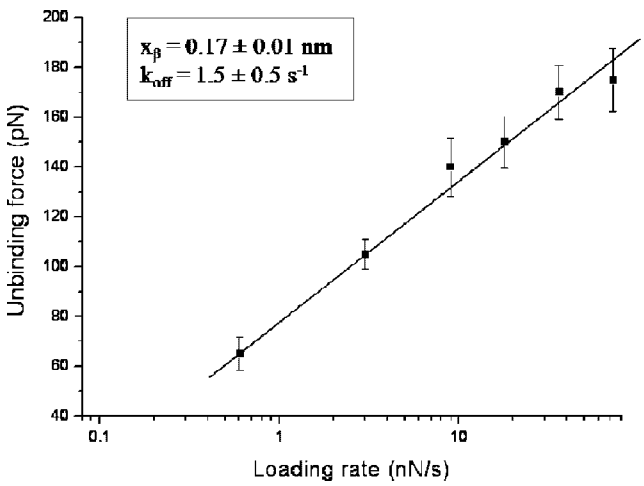

Figure 7. Dynamic force spectrum for the p53/Mdm2 interaction. Plot of the unbinding forces versus the natural logarithm of the different loading rates. The continuous line represents the fit of the experimental data with Bell-Evans model (equation 2). The kinetics parameters obtained are reported in the inset. The uncertainties of force values are given as $\sigma/(N)^{1/2}$, where σ is the standard deviation on N data.

dissociation of the latter to undergo degradation (Haupt *et al*., 1997; Kubbutat *et al*., 1997). Moreover, the k_{off} here estimated is very close to that determined in a stopped-flow fluorimetric study ($k_{off} = 2.0\,s^{-1}$), which has been obtained from the interaction between the two N-terminal domains of both p53 and Mdm2 (Schon *et al*., 2002), where the binding sites of the complex are supposed to be located (Chen *et al*., 1993). Taking into account the striking similarity of the two k_{off} values and, at the same time, the fact that our measured dissociation rate relates to a p53/Mdm2 complex as made up by the full-length proteins, it can be inferred that the two cognate binding sites of the complex undergo a bio-recognition process without any steric hindrance effect from the presence of the entire milieu of the proteins. The occurrence of a specific, dynamical complex between the full-length p53 and Mdm2 proteins, here evidenced for the first time by AFS, adds a new piece of valuable information about the mechanism of p53 regulation.

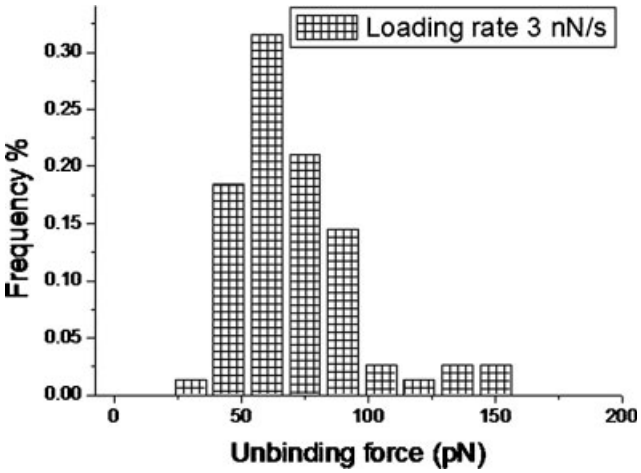

Figure 8. Unbinding force histogram for the p53/azurin interaction.

p53/azurin interaction

Before considering the effect of azurin on the p53/Mdm2 complex, we repeated AFS measurements on p53/azurin system, already studied in a previous work (Taranta *et al*., 2008a), to achieve an inner control, coherent with the present experimental setup. In the previous study, azurin was covalently linked to the AFM tip via one of the two thiol-groups located at the protein surface, a condition that favoured the exposure of the hydrophobic patch to facilitate the binding to p53 (Yamada *et al*., 2002). In the present case instead, azurin was bound to the tip by targeting one of its eleven aminic groups, belonging to lysines exposed on the protein surface. On the other hand, also p53 has been immobilized on the gold substrate with a different strategy with regard to the previous work, according to the protocol illustrated in Figure 1.

Again, we performed thousands of force-distance cycles on different sample positions. The force-curves were recorded at the same approach speed, but varying the retraction velocities to obtain the same loading rate values used for the p53/Mdm2 interaction (0.6–72 nN/s). By processing the curves with the same analysis criteria adopted for the p53/Mdm2 interaction, we obtained a mean unbinding frequency of 14% (at a loading rate of 3 nN/s). This frequency was found to be somewhat lower than that observed in the previous work (19%), due to the random immobilization of azurin in the present case.

All the unbinding force histograms, obtained at the different loading rates, were characterized by clustered distributions. We determined the most probable rupture force from the maximum of the main peak of each force histogram and we found an unbinding force value of 60 ± 5 pN, at a loading rate of 3 nN/s (Figure 8), a value consistent with that reported in the previous work.

Again, the specificity of the unbinding forces and the complex formation was assessed by blocking p53 molecules with a solution of 26 μM azurin and eventually washing the substrate with buffer to remove the unbound azurin. We observed, as a result, a significant reduction from 14 to 6% of the unbinding frequency that was indicative of the specificity of the interactions.

The plot of the unbinding forces versus the natural logarithm of the loading rate (not shown) displayed a linear relationship between the two quantities and provided a k_{off} of $2.4 \pm 1.1\,s^{-1}$.

The k_{off} here obtained indicates that the p53/azurin interaction shows a lower stability than the p53/Mdm2 one: the lifetime of the p53/azurin complex at zero force (τ_0), defined as $1/k_{off}$ (Bell, 1978), results to be, in fact, of 0.4 s, in comparison with 0.7 s for the p53/Mdm2 complex.

p53/Mdm2/azurin competition experiments

As before reported, the formation of a specific p53/Mdm2 complex occurs with the two entire proteins that interact at the level of both their N-terminal domains. On the other hand, azurin can specifically bind to an undetermined region of p53, with its hydrophobic patch. In this respect, it could be very interesting to investigate about a possible competition of azurin with Mdm2 for the same binding site on p53 N-terminus.

In order to probe such a hypothesis, we conceived competitive blocking experiments. The strategy adopted by us is schematically sketched in Figure 9. Firstly, we estimated the frequency of the unbinding events between immobilized p53 and Mdm2 (15%), and then we blocked the substrate with a solution of free azurin, as a possible competitive agent for the p53/Mdm2 interaction (Figure 9A). After washing the substrate, we measured again the unbinding frequency that was found to be almost unchanged after blocking (16%; Figure 9B). To strengthen such a result, we repeated a second blocking experiment in a different protein-combination: we measured the unbinding frequency between immobilized p53 and azurin (14%) and then we blocked the substrate with free Mdm2, by using it as a putative competitor (Figure 9C). Again, after washing, no substantial reduction in the rupture frequency was found (12%; Figure 9D).

These results indicate that no competition is observed between azurin and Mdm2 for the same binding site on p53. From such an evidence and the fact that p53 specifically interacts with both Mdm2 and azurin, it can be inferred that a p53/Mdm2/azurin ternary complex is formed. Very likely, within such complex p53 and Mdm2 would interact by their respective N-terminal domains (Chen *et al*., 1993; Kussie *et al*., 1996), while azurin could bind, through its hydrophobic patch (Yamada *et al*., 2002), to the DBD of p53, as recently proposed by a docking study (De Grandis *et al*., 2007).

We therefore wonder if such a ternary complex might play a functional role. Intriguingly, we could speculate about the possibility that binding of azurin to the p53-DBD could interfere with the ubiquitination process, which is catalyzed by Mdm2 at

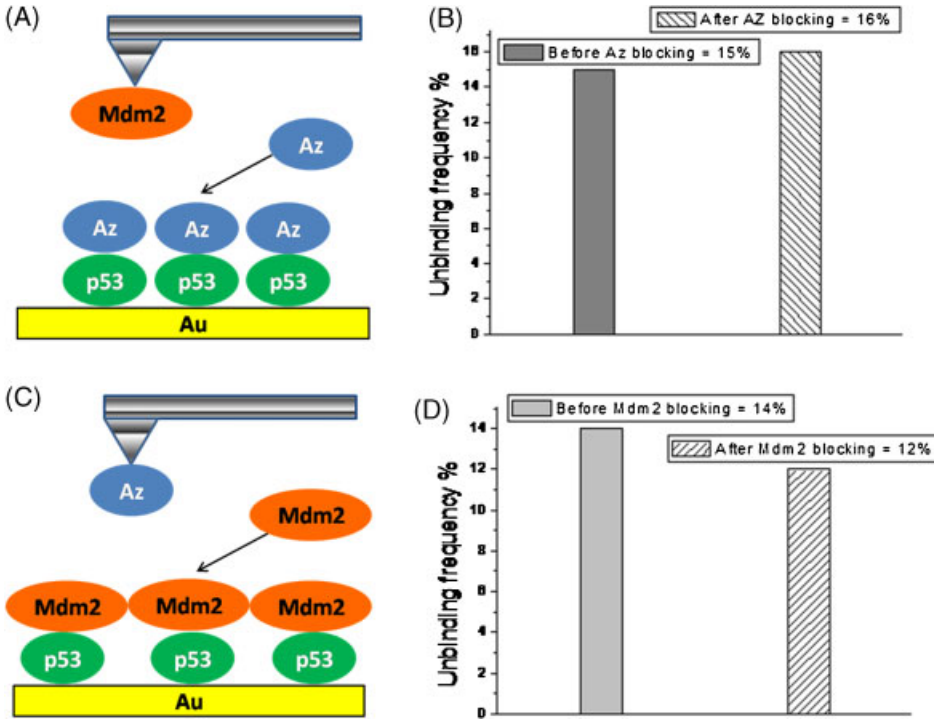

Figure 9. Competitive blocking experiments on the p53/Mdm2/azurin ternary complex. (A) Sketch of the system with azurin used as competitor. (B) Unbinding frequency before and after blocking with azurin. (C) Sketch of the system with Mdm2 used as competitor. (D) Unbinding frequency before and after blocking with Mdm2. All measurements refer to a loading rate of 3 nN/s.

the level of lysine residues located within the p53-DBD (Chan *et al*., 2006), and thus resulting in a steric protection of crucial sites involved in p53 negative regulation (Clegg *et al*., 2008). Undoubtedly, further investigation will be required to assess a possible biological relevance of such a ternary complex.

In conclusion, AFS has proven to be a powerful approach to complement biochemical and bio-molecular information on the p53/Mdm2 interaction. In fact, it allowed us to reach unprecedented kinetic results on the p53/Mdm2 complex formed by the two full-length proteins. Moreover, the AFS study on p53/Mdm2/azurin system has evidenced that the stabilization induced by azurin on p53 cannot be attributed to a competitive binding with respect to Mdm2, for the N-terminal domain of p53. The occurrence of a p53/Mdm2/azurin ternary complex opens a possible new scenario for the anti-cancer action of azurin.

Acknowledgements

All the authors would like to thank Dr. Ada Sacchi (Regina Elena Cancer Institute, Rome; Italy) for useful discussion and suggestions. We are grateful to Prof. Agostina Congiu Castellano and her group for providing circular dichroism equipment. G.F. thanks Dr. Monia Taranta for experimental advises. R. P. is a recipient of a Fellowship from Fondazione Italiana per la Ricerca Sui Cancro (FIRC). The work was partially supported by the PRIN-MIUR 2006 project n. 2006027587.

REFERENCES

Apiyo D, Wittung-Stafshede P. 2005. Unique complex between bacterial azurin and tumour-suppressor protein p53. *Biochem. Biophys. Res. Commun.* **332**: 965–968.

Baumgartner W, Hinterdorfer P, Ness W, Raab A, Vestweber D, Schindler H, Drenckhahn D. 2000. Cadherin interaction probed by atomic force microscopy. *Proc. Natl Acad. Sci. USA* **97**: 4005–4010.

Bell GI. 1978. Models for the specific adhesion of cells to cells. *Science* **200**: 618–627.

Bell S, Klein C, Müller L, Hansen S, Buchner J. 2002. p53 contains large unstructured regions in its native state. *J. Mol. Biol.* **322**: 917–927.

Bonanni B, Bizzarri AR, Cannistraro S. 2006. Optimized biorecognition of cytochrome c 551 and azurin immobilized on thiol-terminated monolayers assembled on Au (111) substrates. *J. Phys. Chem. B* **110**: 14574–14580.

Bonanni B, Kamruzzahan SM, Bizzarri AR, Rankl C, Gruber HJ, Hinterdorfer P, Cannistraro S. 2005. Single molecule recognition between cytochrome c 551 and gold-immobilized azurin by force spectroscopy. *Biophys. J.* **89**: 2783–2791.

Bossi G, Sacchi A. 2007. Restoration of wild-type p53 function in human cancer: relevance for tumour therapy. *Head & Neck* **29**: 272–284.

Chan RY, Mak MC, Fung TK, Lan A, Sin WY, Poon RY. 2006. Ubiquitination of p53 at multiple sites in the DBD—binding domain. *Mol. Cancer Res.* **1**: 15–25.

Chen J, Marechal V, Levine AJ. 1993. Mapping of the p53 and Mdm2 interaction domains. *Mol. Cell. Biol.* **13**: 4107–4114.

Chi SW, Lee SH, Kim DH, Ahn MJ, Kim JS, Woo JY, Torizawa T, Kainosho M, Han KH. 2005. Structural details on Mdm2-p53 interaction. *J. Biol. Chem.* **18**: 38795–38802.

Clegg HV, Itahana K, Zhang Y. 2008. Unlocking the Mdm2/p53 loop. *Cell Cycle* **7**: 1–6.
Dawson R, Muller L, Dehner A, Klein C, Kessler H, Buchner J. 2003. The N-terminal domain of p53 is natively unfolded. *J. Mol. Biol.* **332**: 1131–1141.
De Grandis V, Bizzarri AR, Cannistraro S. 2007. Docking study and free energy simulation of the complex between p53 DNA-binding domain and azurin. *J. Mol. Recognit.* **20**: 215–226.
Ebner A, Hinterdorfer P, Gruber HJ. 2007. Comparison of different aminofunctionalization strategies for attachment of single antibodies to AFM cantilevers. *Ultramicroscopy* **107**: 922–927.
Evans E, Ritchie K. 1997. Dynamic strength of molecular adhesion bonds. *Biophys. J.* **72**: 1541–1555.
Freedman DA, Wu L, Levine AJ. 1999. Functions of the Mdm2 oncoprotein. *Cell. Mol. Life Sci.* **55**: 96–107.
Friddle RW, Sulchek TA, Albrecht H, De Nardo SJ, Noy A. 2007. Counting and breaking individual biological bonds: Force spectroscopy of tethered ligand-receptor pairs. *Current Nanosci.* **3**: 41–48.
Friedsam C, Wehle AK, Kuhner F, Gaub HE. 2003. Dynamic single molecule force spectroscopy: bond rupture analysis with variable spacer length. *J. Phys. Cond. Matt.* **15**: S1709–S1723.
Fuhrmann A, Anselmetti D, Ros R. 2008. Refined procedure of evaluating experimental single-molecule force spectroscopy data. *Phys. Rev.* **E77** 031912: 1–10.
Hanley W, McCarty O, Jadhav S, Tseng Y, Wirtz D, Konstantopoulos K. 2003. Single molecule characterization of P-selectin/Ligand binding. *J. Biol. Chem.* **278**: 10556–10561.
Harris SL, Levine AJ. 2005. The p53 pathway: positive and negative feedback loops. *Oncogene* **24**: 2899–2908.
Haupt Y, Maya R, Kazaz A, Oren M. 1997. Mdm2 promotes the rapid degradation of p53. *Nature* **387**: 296–299.
Hinterdorfer P, Baumgartner W, Gruber HJ, Schilcher K, Schindler H. 1996. Detection and localization of individual antibody-antigen recognition events by atomic force microscopy. *Proc. Natl Acad. Sci. USA* **93**: 3477–3481.
Hinterdorfer P, Dufrêne YF. 2006. Detection and localization of single molecular recognition events using atomic force microscopy. *Nature Meth.* **3**: 347–355.
Hinterdorfer P, Kienberger F, Raab A, Gruber HJ, Baumgartner W, Kada G, Riener C, Wielert-Badt S, Borken C, Schindler H. 2000. Poly (Ethylene Glycol): an ideal spacer for molecular recognition force microscopy/spectroscopy. *Single Mol.* **1**: 99–103.
Honda R, Tanaka H, Yasuda H. 1997. Oncoprotein Mdm2 is an ubiquitin ligase E3 for tumor suppressor p53. *FEBS Lett.* **420**: 25–27.
Hutter JL, Bechhoefer J. 1993. Calibration of atomic-force microscope tips. *Rev. Sci. Instrum.* **64**: 1868–1873.
Janshoff A, Steinem C. 2001. Energy landscapes of ligand-receptor couples probed by dynamic force spectroscopy. *ChemPhysChem* **2**: 577–579.
Kienberger F, Kada G, Gruber HJ, Pastushenko V, Riener C, Trieb M, Knaus HG, Schindler H, Hinterdorfer P. 2000a. Recognition force spectroscopy studies of the NTA-His6 bond. *Single Mol.* **1**: 59–65.
Kienberger F, Pastushenko VP, Kada G, Gruber HJ, Riener C, Schindler H, Hinterdorfer P. 2000b. Static and dynamical properties of single poly (ethylene glycol) molecules investigated by force spectroscopy. *Single Mol.* **1**: 123–128.
Ko LJ, Prives C. 1996. p53: puzzle and paradigm. *Genes Develop.* **10**: 1054–1072.
Kubbutat MH, Jones SN, Vousden KH. 1997. Regulation of p53 stability by Mdm2. *Nature* **387**: 299–303.
Kussie PH, Gorina S, Marechal V, Elenbaas B, Moreau J, Levine AJ, Pavletich NP. 1996. Structure of the Mdm2 oncoprotein bound to the p53 tumor suppressor transactivation domain. *Science* **274**: 948–953.
Lai Z, Auger KR, Manubay CM, Copeland RA. 2000. Thermodynamics of p53 binding to hdm2 (1–126): effects of phosphorylation and p53 peptide length. *Arch. Biochem. Biophys.* **381**: 278–284.
Lavin MF, Gueven N. 2006. The complexity of p53 stabilization and activation. *Cell Death Diff.* **13**: 941–950.
Levine AJ. 1997. p53, the cellular gatekeeper for growth and division. *Cell* **88**: 323–331.
Lim TS, Vedula SR, Kausalya PJ, Hunziker W, Lim CT. 2008. Single-molecular-level study of claudin-1-mediated adhesion. *Langmuir* **24**: 490–495.
Lü S, Ye Z, Zhu C, Long M. 2006. Quantifying the effects of contact duration, loading rate, and approach velocity on P-selectin-PSGL-1 interactions using AFM. *Polymer* **47**: 2539–2547.
Marshall BT, Sarangapani KK, Lou J, McEver RP, Zhu C. 2005. Force history dependence of receptor-ligand dissociation. *Biophys. J.* **88**: 1458–1466.
Merkel R. 2001. Force spectroscopy on single passive biomolecules and single biomolecular bonds. *Physics Reports* **346**: 343–385.
Momand J, Zanbetti GP, Olson DC, George D, Levine AJ. 1992. The Mdm2 oncogene product forms a complex with the p53 protein and inhibits p53-mediated transactivation. *Cell* **69**: 1237–1245.
Oren M. 2003. Decision making by p53: life, death and cancer. *Cell Death Diff.* **10**: 431–442.
Panorchan P, Thompson MS, Davis KJ, Tseng Y, Konstantopoulos K, Wirtz D. 2006. Single molecule analysis of cadherin-mediated cell-cell adhesion. *J. Cell Sci.* **119**: 66–74.
Ratto TV, Langry KC, Rudd RE, Balhorn RL, Allen MJ, McElfresh MW. 2004. Force spectroscopy of the double-tethered concanavalin A mannose bond. *Biophys. J.* **86**: 2430–2437.
Rief M, Grubmüller H. 2002. Force spectroscopy of single biomolecules. *ChemPhysChem* **3**: 255–261.
Roth J, Dobbelstein M, Freedman DA, Shenk T, Levine AJ. 1998. Nucleo-cytoplasmic shuttling of the hdm2 oncoprotein regulates the levels of the p53 protein via a pathway used by the human immunodeficiency virus rev protein. *EMBO J.* **2**: 554–564.
Schon O, Friedler A, Bycroft M, Freund SMV, Fersht AR. 2002. Molecular mechanism of the interaction between Mdm2 and p53. *J. Mol. Biol.* **323**: 491–501.
Sulchek TA, Friddle RW, Langry K, Lau EY, Albrecht H, Ratto TV, DeNardo SJ, Colvin ME, Noy A. 2005. Dynamic force spectroscopy of parallel individual Mucin-1-antibody bonds. *Proc. Natl Acad. Sci. USA* **102**: 16638–16643.
Sulchek T, Friddle RW, Noy A. 2006. Strength of multiple parallel biological bonds. *Biophys. J.* **90**: 4686–4691.
Taranta M, Bizzarri AR, Cannistraro S. 2008a. Probing the interaction between p53 and the bacterial protein azurin by single molecule force spectroscopy. *J. Mol. Recognit.* **21**: 63–70.
Taranta M, Bizzarri AR, Cannistraro S. 2008b. Modelling the interaction between the N-terminal domain of the tumor suppressor p53 and azurin. *J. Mol. Recognit. 22:* 215–222.
Thormann E, Hansen PL, Simonsen AC, Mouritsen OG. 2006. Dynamic force spectroscopy on soft molecular systems: improved analysis of unbinding spectra with varying the linker compliance. *Coll. Surf. B: Bioint.* **53**: 149–156.
Vassilev LT. 2007. Mdm2 inhibitors for cancer therapy. *Trends Mol. Med.* **13**: 23–31.
Vassilev LT, Vu BT, Graves B, Carvajal D, Podlaski F, Filipovic Z, Kong N, Kammlott U, Lukacs C, Klein C, Fotouhi N, Liu EA. 2004. *In vivo* activation of the p53 pathway by small-molecule antagonists of Mdm2. *Science* **303**: 844–848.
Vijgenbbom E, Busch JE, Canters GW. 1997. *In vivo* studies disprove an obligatory role of azurin in denitrification in *Pseudomonas Aeruginosa* and show that azurin expression is under control of RpoS and ANR. *Microbiology* **143**: 2853–2863.
Vogelstein B, Lane D, Levine AJ. 2000. Surfing the p53 network. *Nature* **408**: 307–310.
Wielert-Badt S, Hinterdorfer P, Gruber H, Lin JT, Badt D, Wimmer B, Schindler H, Kinne RK., 2002. Single molecule recognition of protein binding epitopes in brush border membranes by force microscopy. *Biophys. J.* **82**: 2767–2774.
Wiman KG. 2006. Strategies for therapeutic targeting of the p53 pathway in cancer. *Cell Death Diff.* **13**: 921–926.
Yamada T, Goto M, Punj V, Zaborina O, Chen ML, Kimbara K, Majumdar D, Cunningham E, Das Gupta TK, Chakrabarty AM. 2002. Bacterial redox protein azurin, tumour suppressor protein p53, and regression of cancer. *Proc. Natl Acad. Sci. USA* **99**: 14098–14103.
Zhang X, Wojcikiewicz E, Moy VT. 2002. Force spectroscopy of the leukocyte function-associated antigen-1/intercellular adhesion molecule-1 interaction. *Biophys. J.* **83**: 2270–2279.
Zlatanova J, Lindsay SM, Leuba SH. 2000. Single molecule force spectroscopy in biology using the atomic force microscope. *Progress Biophys. Mol. Biol.* **74**: 37–61.

